

Luminescence enhancement and charge transfer band extension in Eu³⁺ doped tungstate and molybdate phosphors

A. Khanna^{a,b} and P.S. Dutta^{a,b,*}

^aSmart Lighting Engineering Research Center, Troy, New York, 12180, USA

^bElectrical Computer and Systems Engineering Rensselaer Polytechnic Institute, Troy, New York, 12180, USA

A_{0.76}WO₄ (A = Ca, Sr, Ba): Eu_{0.24}³⁺, Ca_{0.76}MoO₄: Eu_{0.24}³⁺ and Y_{1.94}MO₆: Eu_{0.06}³⁺ (M = Mo, W) phosphors were synthesized by solid-state reaction and their crystallographic, excitation and emission properties have been compared. Y_{1.94}WO₆: Eu_{0.06}³⁺ and Y_{1.94}MoO₆: Eu_{0.06}³⁺ were found to exhibit charge transfer band (CTB) edge at longer wavelengths compared to their alkaline earth metal tungstate and molybdate phosphors counterparts. This is attributed to the crystal structures of these phosphors. Amongst the alkaline earth metal tungstate phosphors, Ca_{0.76}WO₄: Eu_{0.24}³⁺ exhibits the highest emission intensity. Furthermore, Ca_{0.76}WO₄: Eu_{0.24}³⁺ phosphor crystals grown from high temperature melt shows significant improvement in its emission intensity in comparison to powders synthesized by solid-state reaction.

Key word: Phosphor LEDs, Charge transfer band, Crystal growth, Trivalent europium, Tungstate, Molybdate.

Introduction

Commercial phosphor-converted white LEDs (pc-WLEDs) consist of a blue LED chip and YAG (Y₃Al₅O₁₂: Ce³⁺) phosphor. Since YAG phosphor emission does not cover the entire visible spectrum, these LEDs suffer from poor color-rendering index and high color temperature. pc-WLEDs with high efficacy and superior color rendering properties could significantly benefit from red phosphors with narrow spectral emission [1]. Alkaline earth metal and rare earth tungstates and molybdates serve as excellent host materials for trivalent lanthanide ions like Eu³⁺, which produce narrow emission lines due to f-f transitions. These phosphors are self-activated due to presence of tetrahedral MO₄ (M = Mo, W) groups and absorb energy in the far-UV region, which is efficiently transferred to Eu³⁺ ions [2-5]. Also, these hosts exhibit excellent chemical stability even at elevated temperatures encountered in a typical illumination grade LED. However, due to large band-gap values of these hosts, the charge transfer state is located at high energies. Thus, there is weak absorption (by the host) of light from excitation sources in the 395-465 nm range where high efficiency near UV and blue LEDs are available. The only absorption is due to the Eu³⁺ activator that undergoes narrow f-f transitions leading to weak luminescence with near-UV or Blue LED excitation sources. In order to improve the emission intensity, these phosphors would require strong f-f transitions or charge transfer band (CTB) extension to longer wavelengths. In this study,

the effect of melt crystal growth process and cation size on the intensity of f-f transitions of AWO₄: Eu³⁺ (A = Ca, Sr, Ba) phosphors have been studied. The effect of crystal structure on CTB edge of tungstate and molybdate phosphors has also been reported.

Experimental Details

Solid state synthesis of phosphors

The starting materials used in these experiments were obtained from Alfa Aesar company. The following reactants were used in powder form: Y₂O₃ (99.9% purity), CaO (99.95% purity), SrO (99.5% purity), Ba(NO₃)₂ (99% purity), MoO₃ (99% purity), WO₃ (99.8% purity), Na₂CO₃ (99.5% purity) and Eu₂O₃ (99.9% purity). The powders were weighed by appropriate stoichiometric ratio and ball milled for 30 minutes at 600 rpm using Retsch PM 100 Planetary Ball Mill. After proper mixing, the powders were transferred to quartz crucibles and heated to 1150 °C in the furnace in oxygen ambient. The use of quartz crucibles was found to be satisfactory for the solid-state reaction in contrast to the melt growth wherein the quartz crucibles cracked during high temperature reaction (~1600 °C). For a complete and uniform reaction, the temperature was maintained for 15-24 hours and then the furnace was cooled down to room temperature at a rate of 350 °C/hr. The powders could be extracted out of the crucible in free flowing form.

Melt growth of phosphors

The starting materials were all in dry powder form obtained from Alfa Aesar company. For melt growth, the following reagents were used: CaO (96% purity),

*Corresponding author:
Tel :
Fax:
E-mail: duttap@rpi.edu

Table 1. Phosphor composition and synthesis parameters for melt growth and solid state reaction.

Phosphor Composition	Synthesis Method	Synthesis Temperature (°C)	Cooling Rate (°C/hr)
$\text{M}_{0.76}\text{WO}_4: \text{Eu}^{3+}_{0.12}/\text{Na}^{+}_{0.12}$ (M = Ca, Sr, Ba)	Solid State Reaction	1150	350
$\text{Y}_{1.94}\text{MO}_6: \text{Eu}^{3+}_{0.06}$ (M = Mo, W)	Solid State Reaction	1150	350
$\text{Ca}_{0.76}\text{MO}_4: \text{Eu}^{3+}_{0.24}$ (M = Mo, W)	Solid State Reaction	1150	350
$\text{Ca}_{0.76}\text{WO}_4: \text{Eu}^{3+}_{0.24}$	Melt Growth	1650	2-3

Eu_2O_3 (99.9% purity) and WO_3 (99.8% purity). The initial reactants were weighed by appropriate stoichiometric ratio and ball milled for 30 minutes at 600 rpm. The homogenized powders were then transferred to alumina crucibles and heated to 1650 °C inside a furnace in oxygen ambient. For a complete and uniform reaction, the temperature was maintained for 15-24 hours. Then the furnace was cooled down slowly at 2-3 °C per hour (hr) to 650 °C for nucleation and crystal growth. Thereafter, the furnace was cooled to room temperature at a rate of 350 C/hr. Table 1 summarizes the optimized synthesis and growth parameters for melt growth and solid-state reactions.

Characterization

X-ray diffraction (XRD) data was recorded on Bruker D8 Discover Diffractometer running on Cu $K\alpha$ radiation at 40 kV and 40 mA. This data was used to determine the crystal structure of the synthesized phosphors and to calculate their lattice constants. Excitation spectrum measurements were done using Fluorolog Tau-3 Lifetime Measurement system. Emission spectra were recorded using the Ocean Optics Jazz spectrometer.

Results and Discussion

Crystal structure determination by XRD

The powder XRD patterns are presented in Fig. 1(a-c). Lattice constants calculated from the XRD data are listed in Table 2 wherein the last column presents the standard values of lattice constants taken from JCPDS database. The calculated lattice constants showed little deviation from their ideal values. Furthermore, since all the peaks in the XRD patterns were indexed to the tetragonal structure of AWO_4 (A = Ca, Sr, Ba), CaMoO_4 and monoclinic structure of Y_2MO_6 (M = Mo, W), it is evident that the synthesized phosphors had high phase purity and the Eu^{3+} ions were uniformly incorporated in the lattice.

Excitation spectra of $\text{AWO}_4: \text{Eu}^{3+}$ (A = Ca, Sr, Ba), $\text{CaMoO}_4: \text{Eu}^{3+}$ and $\text{Y}_2\text{MO}_6: \text{Eu}^{3+}$ (M = Mo, W) phosphors

Fig. 2 shows the normalized excitation spectra of

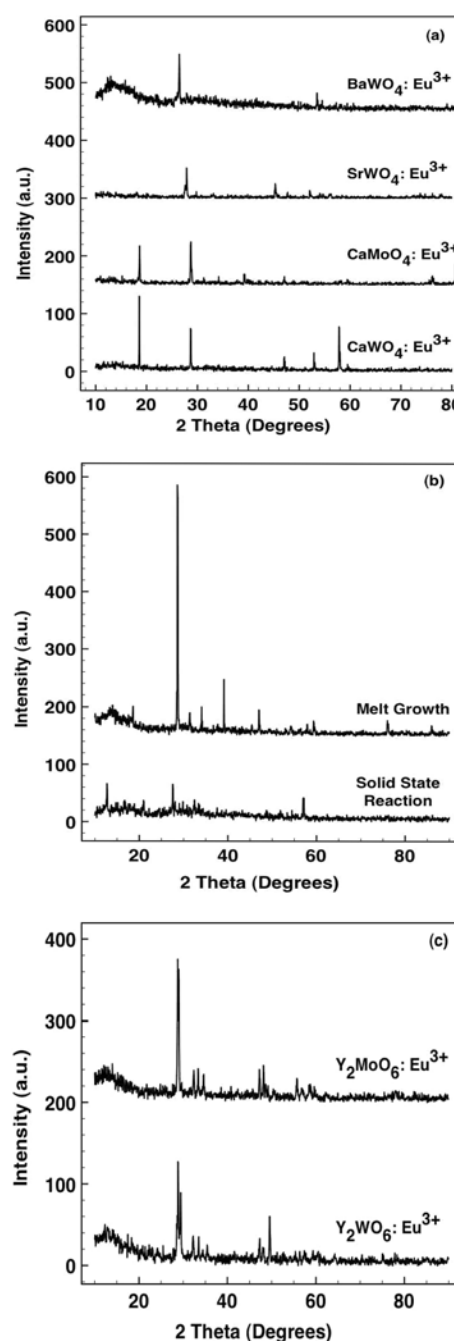
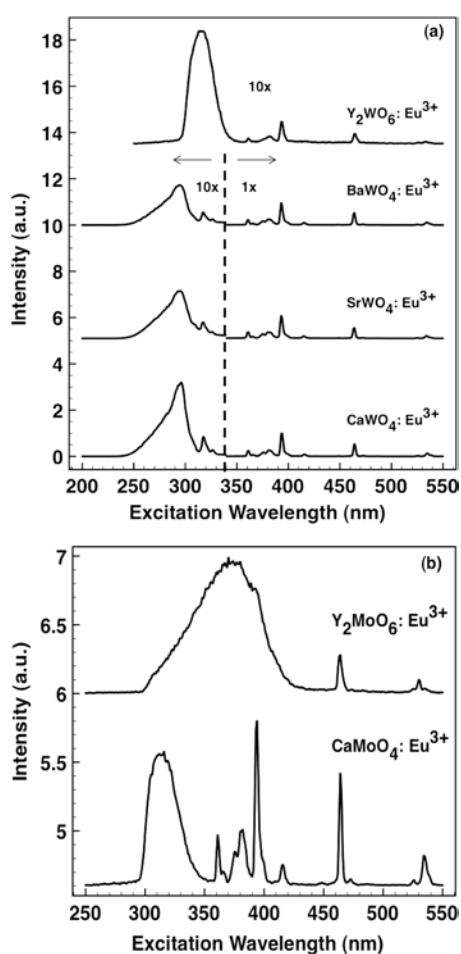


Fig. 1. X-ray diffraction patterns for (a) $\text{A}_{0.76}\text{WO}_4: \text{Eu}^{3+}_{0.12}/\text{Na}^{+}_{0.12}$ (A = Ca, Sr, Ba) and $\text{Ca}_{0.76}\text{MoO}_4: \text{Eu}^{3+}_{0.24}$ synthesized by solid state reaction, (b) $\text{Ca}_{0.76}\text{WO}_4: \text{Eu}^{3+}_{0.24}$ synthesized by solid state reaction and melt grown crystals, (c) $\text{Y}_{1.94}\text{MO}_6: \text{Eu}^{3+}_{0.06}$ (M = Mo, W) synthesized by solid state reaction.

$\text{A}_{0.76}\text{WO}_4$ (A = Ca, Sr, Ba): $\text{Eu}_{0.24}^{3+}$, $\text{Ca}_{0.76}\text{MoO}_4: \text{Eu}_{0.24}^{3+}$ and $\text{Y}_{1.94}\text{MO}_6: \text{Eu}_{0.06}^{3+}$ (M = Mo, W) phosphors monitored at 615 nm emission wavelength. The excitation spectrum of these phosphors comprises a broad band (CTB) and narrow excitation peaks. The broad band in the excitation spectra can be attributed to the charge transfer excitation of $\text{Eu}^{3+}-\text{O}^{2-}$ and $\text{M}^{6+}-\text{O}^{2-}$ (M = Mo, W) bonds and the inter-valence charge transfer (IVCT) between Eu^{3+} and M^{6+} (M = Mo, W) ions. The energy

Table 2. Lattice constants of synthesized phosphors calculated from XRD Data and their comparison with JCPDS Values. *The data in last row is for melt grown crystal.

Phosphor Composition	Crystal Structure	Calculated Lattice Constants				JCPDS Values			
		a (nm)	b (nm)	c (nm)	β ($^\circ$)	a (nm)	b (nm)	c (nm)	β ($^\circ$)
$Y_{1.94}MoO_6: Eu_{0.06}^{3+}$	Monoclinic	1.639	1.103	0.536	109.004	1.639	1.105	0.536	108.49
$Y_{1.94}WO_6: Eu_{0.06}^{3+}$	Monoclinic	0.759	0.536	1.146	106.26	0.759	0.533	1.135	104.41
$Ca_{0.76}MoO_4: Eu_{0.24}^{3+}$	Tetragonal	0.522	0.522	1.156	90	0.533	0.523	1.143	90
$Ca_{0.76}WO_4: Eu_{0.24}^{3+}$	Tetragonal	0.528	0.528	1.123	90	0.524	0.524	1.137	90
$Sr_{0.76}WO_4: Eu_{0.24}^{3+}$	Tetragonal	0.542	0.542	1.156	90	0.542	0.542	1.195	90
$Ba_{0.76}WO_4: Eu_{0.24}^{3+}$	Tetragonal	0.558	0.558	1.073	90	0.561	0.561	1.272	90
* $Ca_{0.76}WO_4: Eu_{0.24}^{3+}$	Tetragonal	0.524	0.524	1.15	90	0.524	0.524	1.137	90

**Fig. 2.** Excitation spectra of (a) $A_{0.76}WO_4: Eu_{0.06}^{3+}/Na_{0.12}^{+}$ ($A = Ca, Sr, Ba$) and $Y_{1.94}WO_6: Eu_{0.06}^{3+}$ phosphors monitored at an emission wavelength of 615 nm, (b) Excitation spectra of $Ca_{0.76}MoO_4: Eu_{0.24}^{3+}$ and $Y_{1.94}MoO_6: Eu_{0.06}^{3+}$ phosphors monitored at an emission wavelength of 615 nm. Relative magnifications used in (a) are indicated next to the curves.

of charge transfer excitation depends upon the co-valency of the $Eu^{3+}-O^{2-}$ and $M^{6+}-O^{2-}$ ($M = Mo, W$) bonds. Higher co-valency leads to lower energy. The photoluminescence pathway is described in reference 6. The narrow excitation peaks originate from Eu^{3+} f-f transitions.

Table 3. Comparison of emission intensities of $MWO_4: Eu^{3+}$ ($M = Ca, Sr, Ba$), $CaMoO_4: Eu^{3+}$ and $Y_2MO_6: Eu^{3+}$ ($M = Mo, W$). *The data in last row is for melt grown crystal.

Phosphor Composition	Cation Size (pm)	CTB Edge (nm)	Relative Intensity with 395 nm Excitation	Relative Intensity with 465 nm Excitation
$Y_{1.94}MoO_6: Eu_{0.06}^{3+}$	104	400	10.62	5.6
$Ca_{0.76}MoO_4: Eu_{0.24}^{3+}$	114	330	16.6	4.66
$Y_{1.94}WO_6: Eu_{0.06}^{3+}$	104	330	3.717	2.52
$Ca_{0.76}WO_4: Eu_{0.24}^{3+}$	114	320	7.3	3.4
$Sr_{0.76}WO_4: Eu_{0.24}^{3+}$	132	320	2.8	2.1
$Ba_{0.76}WO_4: Eu_{0.24}^{3+}$	135	320	1	1
* $Ca_{0.76}WO_4: Eu_{0.24}^{3+}$	114	320	16.68	5.67

Table 3 provides the comparison of emission intensities of $A_{0.76}WO_4: Eu_{0.24}^{3+}$, $Ca_{0.76}MoO_4: Eu_{0.24}^{3+}$ and $Y_{1.94}MoO_6: Eu_{0.06}^{3+}$ ($M = Mo, W$) phosphors. It is seen that $Y_{1.94}MoO_6: Eu_{0.06}^{3+}$ and $Y_{1.94}WO_6: Eu_{0.06}^{3+}$ CTB edges are at longer wavelengths compared to the alkaline earth metal molybdate and tungstate, respectively. This is attributed to the monoclinic structure of yttrium molybdate and tungstate as opposed to tetragonal structure of alkaline earth metal tungstates and molybdates. In the tetragonal and monoclinic systems, M^{6+} ($M = Mo, W$) ion is surrounded by four and six O^{2-} ions, respectively. A higher co-ordination number results in a longer $M^{6+}-O^{2-}$ (Mo, W) bond and thus a lower CTB energy. In references 7 and 8, it has been reported that orthorhombic yttrium tungstate and molybdate $Y_{2-x}(MO_4)_3: Eu_x^{3+}$, $M = Mo, W$ phosphors with tetrahedral coordination of transition metal ion exhibit CTB edge at shorter wavelengths as compared to the monoclinic yttrium molybdate and tungstate ($Y_{1.94}MoO_6: Eu_{0.06}^{3+}$, $M = Mo, W$) phosphors with octahedral coordination of transition metal ion. Furthermore, it is clear from data in Table 3 that of all the alkaline earth metal cations, Ca^{2+} based tungstate phosphors exhibited the highest emission intensity. This is explained in terms of the difference between the ionic radii of alkaline earth

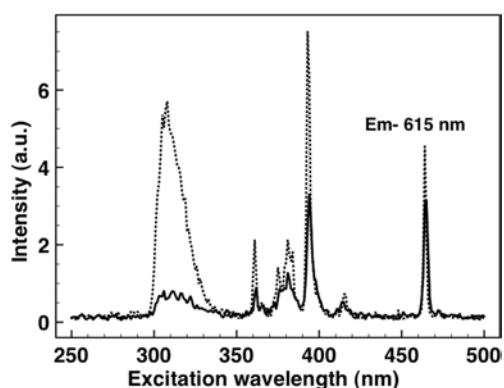


Fig. 3. Excitation spectra of $\text{Ca}_{0.76}\text{WO}_4:\text{Eu}^{3+}_{0.24}$ monitored at an emission wavelength of 615 nm. Solid curve is for samples prepared by solid state reaction and dotted curve is for melt grown crystals.

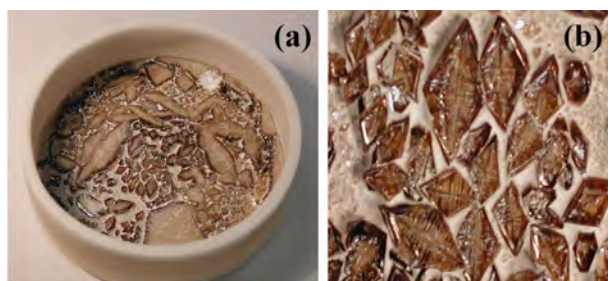


Fig. 4. (a) Melt grown crystals of $\text{Ca}_{0.76}\text{WO}_4:\text{Eu}^{3+}_{0.24}$ in the alumina crucible (crucible diameter: 50 mm), (b) magnified view of the smaller crystals (length ~ 5 - 7 mm).

metal cations and Eu^{3+} ions. Since, Eu^{3+} replaces alkaline earth metal cations in the lattice, a smaller mismatch between the size of these ions results in better solid solubility and thus, better incorporation of Eu^{3+} dopant ions in the lattice. Ca^{2+} (114 pm) is closest in size to Eu^{3+} (109 pm) leading to a higher concentration of dopants in the lattice sites of calcium based phosphors and higher emission intensity.

Effect of melt growth process on excitation spectrum of $\text{CaWO}_4:\text{Eu}^{3+}$ phosphors

Fig. 3 shows the effect of melt growth on phosphor excitation spectrum. The emission intensity of $\text{Ca}_{0.76}\text{WO}_4:\text{Eu}_{0.24}^{3+}$ phosphor prepared by melt growth is approximately 2.3 and 1.7 times the intensity of $\text{Ca}_{0.76}\text{WO}_4:\text{Eu}_{0.24}^{3+}$ phosphor prepared by solid state reaction with 395 nm and 465 nm excitations, respectively. Melt crystal growth provides superior crystal quality. In addition, higher growth temperature leads to better incorporation and activation of dopants in the lattice. Fig. 4 shows typical crystals (few mm in dimensions) grown from melt.

Conclusions

Alkaline earth metal and rare earth molybdates and tungstates are good candidates for red phosphors with narrow spectral emission and hence are suitable for enhancing color rendering index and efficacy of phosphor converted white LEDs. Melt growth of these phosphors doped with Eu^{3+} ions led to improved emission intensity as compared to powders obtained through solid-state reaction. The improvement was attributed to high crystal quality of the single crystal phosphors and better incorporation of dopants into the host lattice in the melt grown phosphors. Phosphor single crystals will also help reduce scattering losses (due to powder based phosphor particles) in LED packages. Rare earth monoclinic $\text{Y}_{1.94}\text{MO}_6:\text{Eu}_{0.06}^{3+}$ ($\text{M} = \text{Mo}, \text{W}$) phosphors exhibited a longer CTB edge than the tetragonal alkaline earth metal molybdates and tungstates, respectively. Amongst the alkaline earth metal tungstate phosphors, $\text{Ca}_{0.76}\text{WO}_4:\text{Eu}_{0.24}^{3+}$ exhibited the highest emission intensity at 395 nm and 465 nm excitation wavelengths on account of similar ionic radii of Ca^{2+} and Eu^{3+} which possibly results in higher solid solubility and better incorporation of activator in the lattice site.

Acknowledgements

This work was supported by the National Science Foundation (NSF) Smart Lighting Engineering Research Center (ERC) under Cooperative Agreement EEC-0812056 and by New York State Foundation for Science, Technology and Innovation (NYSTAR) under contracts C080145 and C090145.

References

1. J.Y. Tsao, M.E. Coltrin, M.H. Crawford, and J.A. Simmons, Proc. of the IEEE 98 [7] (2010) 1162-1179.
2. Y. Hua, W. Zhuang, H. Ye, D. Wang, S. Zhang, and X. Huang, J. Alloys Compd. 390 [133] (2005) 226-229.
3. E. Cavalli, E. Bovero, and Alessandro Belletti, J. Condens. Matter. Phys. 14 (2002) 5221-5228.
4. M.V. Nazarov, D.Y. Jeon, J.H. Kang, E.-J. Popovici, L.-E. Muresan, M.V. Zamoryanskaya, and B.S. Tsukerblat, Solid State Commun. 131 [5] (2004) 307-311.
5. A. Xie, X. Yuan, S. Hai, J. Wang, F. Wang, and L. Li, J. Phys. D: Appl. Phys. 42 (2009) 105107-105114.
6. P. Dorenbos, A.H. Krumpel, E. Kolk, P. Boutinaud, M. Bettinelli, and E. Cavalli, Opt. Mater. 32 [12] (2010) 1681-1685.
7. S. Wang, K.K. Rao, Y. Wang, Y. Hsu, S. Chen, and Y. Lu, J. Am. Ceram. Soc. 92 [8] (2009) 1732-1738.
8. T. Kano, S. Seki, and S.Z. Chiou, J. Lumin. 29 [2] (1984) 163-176.